Surface Modification of AISI 316L Stainless Steel by Oxynitrocarburizing for Solar Collector Applications

Gregorio Vargas[1], Lizsandra López[1] and Aldo. F. Chávez[1]

[1] Centro de Investigación y de Estudios Avanzados del IPN, Saltillo (México)

Abstract

The surface modification of AISI 316L stainless steel was studied using a mixture of cyanate and sodium carbonate salts. This mixture was placed in paste form on previously polished steel substrates. The oxinitrocarburizing treatment was carried out at 580 °C for 5 to 20 minutes by the eutectic mixture paste of sodium cyanate (NaCNO) and sodium carbonate (Na_2CO_3) salts. Characterization of the materials was carried out using XRD, SEM/EDS, UV/Vis, FT-IR spectroscopy techniques. The oxynitrocarburizing time played an important role in the surface modification of the stainless steel, in terms of the nature of the phases formed in the resulting oxidized and nitrided layers, thickness of both layers and surface optical properties of the treated samples. The development of a thick surface oxidized layer was detrimental for the surface optical properties of the samples. In this sense, a 5 min oxynitrocarburizing treatment produced the best results. The best optical properties obtained at the surface of the steel were an absorptance (α) of 0.90 and an emittance (ε) of 0.1.

Keywords: surface modification, thermochemical treatment, pastes, optical properties.

1. Introduction

Spectrally selective surfaces for applications in solar thermal collectors should have high absorptance (α) values in the visible spectrum region and low emittance (ε) in the infrared region [Tian and Zhao 2013, Thirugnanasambandam et al 2010]. A more specific way to evaluate the spectral selectivity is to calculate the relationship between solar absorptivity and thermal emittance (α/ε). However, this method is considered inappropriate for evaluating the photothermal conversion efficiency. For example, a solar absorber with a solar absorptivity of 0.60 and a thermal emittance of 0.03 achieves a ratio of 20 but does not have a higher photothermal conversion efficiency than an absorber with a solar absorptance of 0.90 and a thermal emittance of 0.1 that achieves a ratio of only 9. To classify the spectral selectivity and, therefore, the performance of a solar absorber, the expression α-0.5ε is used to reflect the weight factor of the thermal emittance in a more reasonable way according to ISO 22975-3 [Caliari and Timelli 2015].

Currently there is a wide variety of surface modification technologies aimed at improving the functional properties of metal alloys. Many of these technologies have already been tested industrially but their initial investment, the degree of control required, their maintenance and operation expenses and their interaction with the environment prevent their widespread dissemination. There is a continuous effort to improve the existing technologies and to search for novel treatments to improve the performance of the surface functionality. A selection of the optimal technique depends on the capability, the economics and easiness of scaling up of the process, the size characteristics and geometry of the component to be modified or coated, their functionality requirements. The environmental aspect has also become a driver of new technological requirements.

The surface blackening of stainless steels is among the spectrally selective surfaces that meet the main requirements. Electroplating is one of the more suitable coating techniques employed by the solar thermal industry for over 50 years. Chemical conversion, spray pyrolysis, vacuum deposition, and chemical vapor deposition are the other common coating techniques [Wijewardane and Goswami 2012]. Surface modification of steels by thermochemical treatments has been commonly used to improve their wear properties, hardness and corrosion resistance; however, the effect of the oxynitrocarburizing processes on the surface optical properties of stainless steels, have not been reported for their application in solar collectors. Besides the formation of stable nitrides occurring during the salt oxynitrocarburizing of a stainless steel, the formation of a black, dense and thermally stable oxide layer could be

doi:10.18086/eurosun2018.10.11 Available at http://proceedings.ises.org

formed on top of the nitride layer. The characteristics of this two-layered coating configuration could be tailored to obtain the surface optical properties required for applications in solar collectors.

In this sense, the present work was aimed to obtain a spectrally selective surface on AISI 316L Stainless Steel for its application in solar collectors. This innovative method allows homogeneous and uniform modified surfaces in short times using a self-protective diffusion paste. Depending on the ingredients, the paste can diffuse different elements such as nitrogen on the surface of a material to harden and protect the surface against corrosion or modify its optical properties. The main advantages of the self-protecting pastes in thermochemical treatment of metals are:

- No protective atmosphere is required during the heat treatment,
- They are easy to handle and quick to prepare,
- They are suitable for the partial or selective treatment of a surface
- The thermochemical treatments can be done in a wide variety of conventional ovens.
- With respect to molten salts, this method substantially increases the performance of the reagents and radically decreases the disposal of waste or the regeneration of the salts.
- The treatment can be carried out at lower temperatures because the melting state is not required.

In the nitrocarburized materials, a “compound layer”, comprised by iron and chromium nitrides and iron carbide, is commonly formed at the outermost zone of the substrate surface, while a “diffusion zone”, comprising a solid solution of nitrogen in the base alloy, is formed just underneath the latter layer. In the “oxy-nitrocarburizing” processes, the steel is subjected to an additional post-oxidation stage [Thirugnanasambandam 2010]. The post-oxidation is used to create a layer of Fe_3O_4 on top of the compound layer [Caliari and Timelli 2015]. The simultaneous oxidation and nitriding of steel in a single treatment is not common [Grabke et al 2003]; oxidation of the workpiece is commonly considered detrimental and thus it is usually avoided during the nitriding process. However, to generate spectrally selective black coatings our process uses a single and relatively short treatment cycle, without the post oxidative treatment.

2. Experimental method

The composition of the steel used was analyzed by atomic emission spectroscopy (AES). Its chemical composition is indicated by Table 1.

Table 1. Chemical Composition of AISI 316L Stainless Steel

C	Si	Mn	P	S	Cr	Mo	Ni	Al	Cu	Nb	Ti	V	W
0.013	0.234	1.63	0.06	0.022	16.69	2.06	9.7	0.0005	0.48	0.0002	0.007	0.082	0.073

The steel specimens were polished at a mirror level, then subjected to an ultrasonic cleaning procedure. The paste was formed using a mixture of NaCNO and Na2CO3 salts with carboxymethyl cellulose as a binder. The oxynitrocarburizing treatment was carried out at 580 °C for 5 to 20 minutes. The XRD analyses were carried out directly on the treated surface of the samples, without any prior preparation, using for this a Bruker AXS D8 Advance XRD apparatus, with monochromated CuKα radiation, voltage of 40 KV, current density of 30 mA, and a step size of 0.02° (2θ) per second. For the SEM/EDS analyses, the treated samples were cross-sectioned. Then, the samples were hot mounted in resin with the cut surface facing downwards. This surface was then metallographically prepared with a final polish using a colloidal silica suspension with a particle size of 0.04 µm. Then, the metallographically prepared surfaces of the samples were etched for a minimum of 20 s using glyceregia etchant at room temperature and observed and analyzed by using a PHILIPS XL30ESEM scanning electron microscope, employing for this an acceleration voltage of 20 keV. The optical properties of the treated surfaces were evaluated by UV/Vis and FT-IR spectroscopy techniques, using for this a LAMBDA 350 UV/Vis Spectrophotometer and a Frontier FT-IR spectrometer, respectively, both from PerkinElmer. The UV/Vis Spectrophotometer was fitted with a 150 mm integrating sphere, which allowed us to obtain the spectral reflectance of the samples in the solar radiation wavelength range. The FT-IR spectrometer was fitted with a diffuse reflectance accessory, which allowed us to obtain the near-infrared (NIR) spectral reflectance of the samples.

The solar absorptance (α) and the thermal emittance (ε) of the nitrided materials were determined using the procedure described by [Li 2000], taking the required solar irradiance values from the ASTM G173-03.

3. Results and discussion

Phase Evolution. The XRD (Figure 1) studies, together with the EDS spectra and the microstructure of Figure 2 obtained by SEM, revealed that the compound layer was a double-layered zone. The layer located at the outermost zone of the samples was composed by intermixed crystals of Fe_3O_4, and ε-Fe_3N, with increasing relative proportions of the first phase and decreasing relative proportions of the second phase with increasing treatment time.

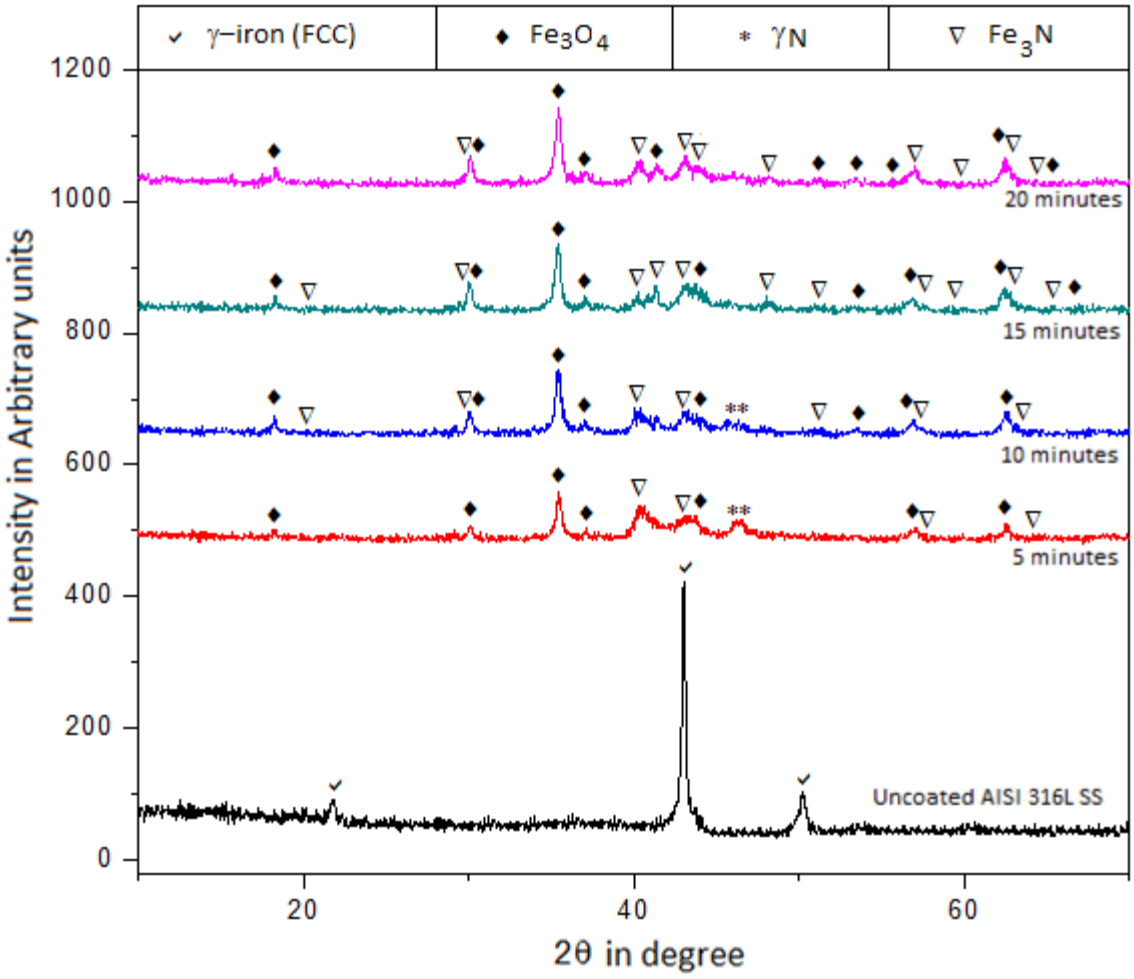

Figure 1 XRD analysis of Stainless Steel 316L before and after thermochemical treatments at 580ºC during 5, 10, 15 y 20 minutes

In the XRD pattern obtained for the sample treated for 20 minutes we can see the presence of a single, relatively short and broad, diffraction peak centered at ~43°. This peak was assigned to the Fe_3O_4 and ε-Fe_3N phases. It is well known that the intensity of the XRD peaks can be affected, among other things, by the crystallite size and by the occurrence of "preferred orientation" phenomenon. Smaller crystallite size causes peaks being lower and wider, while preferred orientation may cause the peaks of some planes becoming unusually tall. The broad peaks located at 44° and 46° for the samples treated for 5 and 10 minutes were ascribed to expanded austenite (γN).

The thickness of the compound layer, as well as that of the diffusion zone, increased with increasing treatment time. Our results confirm that two different phenomena, oxidation and nitrocarburizing, took place in parallel at the surface of the stainless-steel substrates immersed in the salt bath at 580 °C for different times.

Formation of the oxidized compound layer. Figure 2 shows the microstructure of an AISI 316L sample after thermochemical treatment of 20 minutes at 580ºC. Shortly after heating at 580ºC, the salt paste contains Na^+, CO_3^{2-}, CN^-, N, C, O^{2-}, CO and CO_2 chemical species. Later, highly reactive and oxidizing peroxide ions (O_2^{2-}) started to be continuously produced by reaction of the salt with O_2 from the air atmosphere, which is practically insoluble in the bath at ~600 °C [Andresen 1979; Frangini and Scaccia 2004, 2014; Appleby and Nicholson 1972]. Then, the O^{2-} and

O_2^{2-} ions reacted with the Cr_2O_3 surface film of the samples to form Na_2CrO_4 [Spiegel et al 1997; Salih et al 2001], which is very soluble in the molten salt [Mehlig 1936; Biedenkopf et al 2000]. This significantly diminished the corrosion resistance of the stainless steel [Pettersson et al 2011a, 2011b]. This oxide is a p-type metal-deficient (with excess oxygen) non-stoichiometric semiconductor [Schmalzred 1986; Danielewski 2003; Bhat 2018], in which the oxygen atoms are practically immobile while the metal atoms can easily move through the cation vacancies (predominant defects) [Craig 1991]. When this kind of oxides are exposed to an oxidation potential gradient, a flux of cation vacancies is established from the side with the highest oxidation potential (substrate/bath interface) toward the side with the lowest oxidation potential (compound layer/diffusion zone interface), with a simultaneous flux of cation ions (Fe) in the opposite direction [Vedula 1987]. On reaching the sample surface, the diffused Fe reacts with the O^{2-} and O_2^{2-} ions from the salt bath, forming a layer of Fe_3O_4 on top of the previous layer. The Fe_3O_4 is chemically compatible with the molten salt, and it is also the most stable phase at the highest oxidation potential conditions found at the substrate / bath interface [Davies and Dinsdale 2005].

Part of the diffused Fe that reaches the sample surface reacts with C and N coming from the salt, forming ε-Fe_3N and creating a zone with intermixed crystals of both phases and Fe_3O_4 at the outermost region of the compound layer. Since carbon has a very low solubility and diffusivity in Fe_3O_4 [Grabke and Wolf 1987; Wolf and Grabke 1988; Bonnet et al 2003], it could not go deeper into the sample surface. In contrast, since Fe_3O_4 is permeable to nitrogen [Schaaf and Landry 1998], also shows the same behavior, the continuous diffusion of nitrogen into the steel matrix was not hindered. The formation of ε-Fe_3N was promoted by the presence of carbon and oxygen ion species at that site [Schaaf and Landry 1998; Pye 2003].

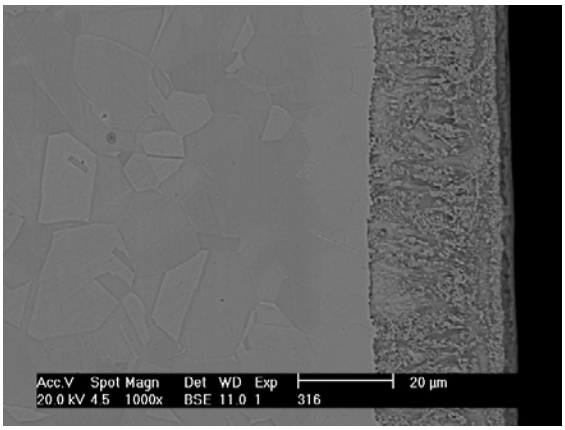

Figure 2 Microstructure of AISI 316L after thermochemical treatment of 20 minutes at 580ºC

Formation of the diffusion zone. The diffusion zone was mainly composed by nitrogen solid solution in austenite, with a small amount of CrN also present in it for the case of the samples treated for times longer than 5 minutes.

The fact that the diffusion zone showed a considerable growth, even after the compound layer was formed, indicates that the latter layer did not hinder the diffusion of nitrogen into the steel matrix. As already mentioned, Fe_3O_4 is permeable to nitrogen [Schaaf and Landry 1998], and since $FeCr_2O_4$ has the same structure, it may also have a similar behavior, although related information was not found in the published literature. It is also known that the formation of Fe_3O_4 results in a significant increase in the substrate surface area, and that this promotes the nitrogen uptake; ε-Fe_3N also allows the diffusion of nitrogen, although to a lesser extent with respect to other iron nitrides and Fe_3O_4 [Hosseini et al 2010]. Fe_3C acts as a diffusion barrier for both carbon and nitrogen [Nikolussi et al 2010]. Thus, except for the latter phase, all the other phases that were present in the compound layer allowed a relatively easy diffusion of nitrogen into the steel matrix. However, an additional factor that must be considered is the diffusion of nitrogen through the grain boundaries and extended defects that were present at that site. This explains why the Fe_3C phase also did not hinder the diffusion of nitrogen into the steel matrix, although it could be expected to do so.

The "expanded austenite" phase, also known as γN phase, was formed in the samples treated for 5 and 10 minutes, which indicates that this phase was developed initially but it rapidly decomposed into CrN and austenite [Manova et al 2016; Wang et al 2012; Chistiansen and Somers 2006]. This also agrees with previous literature reports [Fernandes et al 2012; Williamson et al 1991], in which it was mentioned that expanded austenite can be formed after relatively short times at ~450-600 °C. It has been reported [Mändl et al 2003] that this phase is usually formed at 350-400 °C in nitrided austenitic stainless steels, with a nitrogen content in interstitial solid solution varying from 5 to 30 at. %, which causes an expansion of up to 13% of the austenite crystal lattice. The formation of this phase

has also been reported during the salt bath nitriding of 304 austenitic stainless steel at 570 °C for 2 h [Monteiro et al 2017]. This leads to the development of compressive stresses near the sample surface [Tkacz-Śmiech et al 2016], with a corresponding increase in its hardness, wear resistance, strength and toughness [Williamson et al 1991; Mändl et al 2003; Monteiro et al 2017; Tkacz-Śmiech et al 2016; Manova et al 2017].

To confirm the diffusion of nitrogen in the steel, a line scan by EDS analysis was carried out for the samples of each treated times (See micrographs of Figure 3).

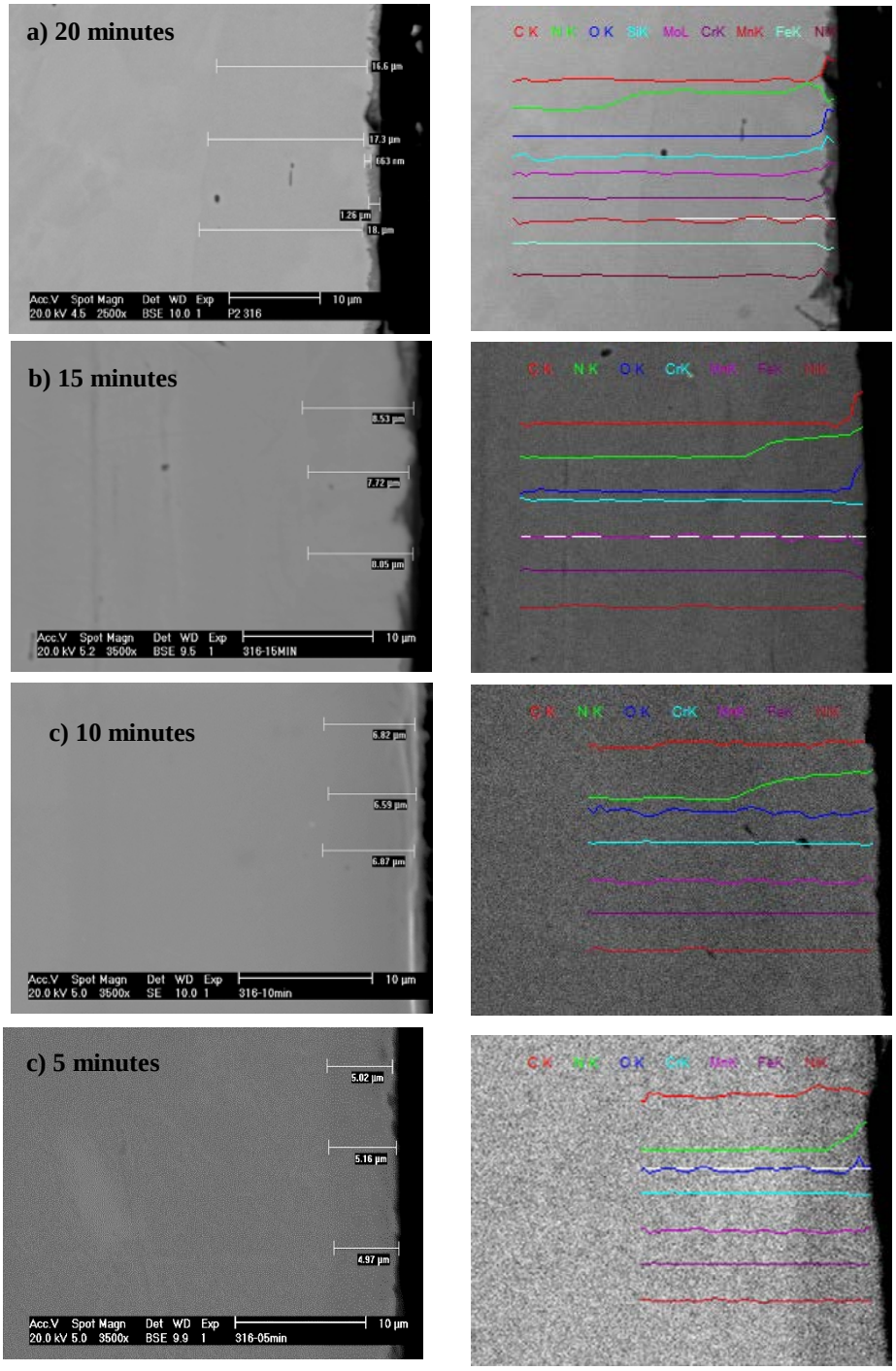

Figure 3. Micrographs and Line scans by EDS of AISI 316L steel samples treated at 580 °C for: a) 20min, b) 15min, c) 10min and d) 5min

Surface optical properties of the treated samples. The thermochemical processes like the one employed in this work have not been used with the purpose of modifying the surface optical properties of austenitic stainless steels, they have only been used to improve their wear resistance, hardness and corrosion resistance [Mittemeijer 2013]. The black appearance of the samples obtained by the oxynitrocarburized samples was the reason that motivated us

to investigate the possibility of using the oxynitrocarburized AISI 316L stainless steel for potential applications in solar collectors.

Table 2 shows the values of α and ε determined by UV/Vis and FT-IR spectroscopy techniques for the oxy-nitrocarburized samples. During the first 20 minutes, the value of α tended to increase with increasing treatment time; longer treatment times made no significant difference on the value of this property. On the other hand, the lower value of ε were obtained with the shorter processing table 2 shows that the material treated for 5 minutes achieved a selectivity ratio of 0.85, as well as solar absorptance and thermal emittance values of 0.90 and 0.10, respectively, which were the closest ones to the ideal values. The thermal emittance obtained for this material was close to that reported for black chrome electrodeposited coatings [Hutchins 1983].

We surmised that the combination of Fe_3O_4, γN and Fe_3C phases formed at the substrate surface after 5 minutes of treatment, as well as the configuration of the oxidized compound layer achieved under such conditions, mainly regarding the small thickness of the latter, were responsible for the best surface optical properties obtained for this sample. The surface optical properties of the substrates were negatively affected by the larger relative proportions of Fe_3C and Fe_3O_4, formed at the outermost zone of the compound layer with longer treatment times, along with the simultaneous thickening of this layer occurring under such conditions. All these factors led to an unwanted increase in the thermal emittance of the treated samples. This is supported by the similarity shown by the behavior of the optical properties of our treated samples with respect to those of the two-layered coating configuration mentioned in the literature [Hutchins 1983], in which an absorbing layer is combined with a reflecting layer. The absorbing layer might be a dielectric semiconductor, such as the oxides of various metals, while the reflecting layer is usually a metal with high IR reflectivity, which in certain cases can be the substrate itself. The absorbing layer has a typical thickness of ~1 μm, which is much shorter than the peak wavelength of emission of a black body. Under these conditions, the absorber is transparent to the IR radiation, allowing the reflecting layer to be "seen" by the incoming radiation, minimizing in this way the thermal emittance of the combination. Thus, the coating configuration and thickness have a great influence on the spectrally selective properties of the material surface. In our case, the absorptance gradually increased with increasing thickness of the compound layer, which gradually became mostly formed by semiconductor spinel-type oxides.

With the development of this work we intended to offer an alternative way to modify the surface optical properties of AISI 316L stainless steel for potential applications in solar collectors. Other well-established ways to do this exist, but the procedure used by us could offer some advantages, such as use of simpler and cheaper equipment, easier process to scaling up and operation, and lower overall operational costs.

Table 2: Oxynitrocarburizing Time Effect on Optical Properties of AISI 316L SS Surface at 580°C

Treatment Time (minutes)	Emittance (ε)	Absorptance (α)
20	0.30	0.93
15	0.20	0.90
10	0.15	0.90
5	0.10	0.90

According to table 2, the oxynitrocarburizing time played an important role in the surface modification of the stainless steel in terms of surface optical properties of the treated samples. The development of a thick surface oxidized layer was detrimental for the surface emittance of the samples. In this sense, a 5 min oxynitrocarburizing treatment produced the best results. According to microstructural characterization two different layers were developed at the surface of the treated samples, especially with treatment times longer than 5 minutes. These were an outermost oxidized layer, underneath which a nitrided layer was formed. After 5 minutes of treatment, both layers were very thin and without a clear separation existing between them. The phases formed in this case were a Fe-Cr spinel oxide, Fe_3O_4, Fe_3C, and γN, and probably a solid solution of N in Fe. With treatment times longer than 5 minutes, both zones became wider and perfectly distinguishable from each other, with a growth rate much faster for the nitrided layer than for the oxidized layer, with diffusion control in the first case and with a likely reaction control in the second. For these treatment times, the oxidized layer became composed by Fe_3O_4, and Fe_3N, while the nitrided zone was composed by a solid solution of N in Fe and γN.

4. Conclusions

We studied the surface microstructural evolution of AISI 316L stainless steel oxy-nitrocarburized from 5 to 20 minutes at 580 °C using a salt paste based on the eutectic composition of the system $NaCNO\text{-}Na_2CO_3$. Simultaneous oxidation and nitrocarburizing of the sample surface took place during the thermochemical treatments, with formation of an outermost oxidized compound layer under which a nitrided diffusion zone was developed. Two different sublayers were developed at the compound layer, which was more evident for treatment times longer than 5 minutes. The outermost sublayer was composed by a mixture of Fe_3O_4, and γN phases, with increasing relative proportions of Fe_3O_4 and decreasing relative proportions of γN, with increasing treatment time.

The material treated for 5 minutes was found to be better for potential applications in solar collectors. This material showed a solar absorptance of 0.90, a thermal emittance of 0.10, and a selectivity factor $(\alpha\text{-}0.5\varepsilon)$ of 0.85, which were relatively close to those of good spectrally selective solar absorber.

Acknowledgements

This work was supported by the Mexican Center for Innovation in Solar Energy (CeMIE-Sol), Renewable Energy Institute of the Mexican National University (IER-UNAM) [CONACYT-SENER-Energy Sustainability Sectorial Fund, Strategic Project No. P-18]; APGM gratefully acknowledges a PhD scholarship granted by CONACYT.

5. References

Andresen A.E., 1979. Solubility of oxygen and sulfur dioxide in molten sodium sulfate and oxygen and carbon dioxide in molten sodium carbonate, J. Electrochem. Soc. 126, 328-334.

Appleby A.J., 1972. Nicholson S.J., Oxygen reduction in carbonate melts: Significance of the peroxide and superoxide ions, J. Electroanal. Chem. Interfacial Electrochem. 38, 13-18.

ASTM G173-03., 2012. Standard Tables for Reference Solar Spectral Irradiances.

Bhat S., 2018. The desired features of an oxide film on stainless steel tubing, Mater. Perform. 57, 40-43.

Biedenkopf P., M. Bischoff M., Wochner T., 2000. Corrosion phenomena of alloys and electrode materials in Molten Carbonate Fuel Cells, Mater. Corros. 51, 287-302.

Bonnet F., Ropital F., Berthier Y., Marcus P., 2003. Filamentous carbon formation caused by catalytic metal particles from iron oxide, Mater. Corros. 54, 870-880.

Caliari D., Timelli G., 2015. An investigation into the effects of different oxy-nitrocarburizing conditions on hardness profiles and corrosion behaviour of 16MnCr5 Steels, Int. J. Metall. Mater. Eng. 110, 1-9.

Christiansen T., Somers M.A.J., 2006. Decomposition kinetics of expanded austenite with high nitrogen contents, Z. Metallkd. 97, 79-88

Craig B.D., 1991. Fundamental Aspects of Corrosion Films in Corrosion Science, Springer Science & Business Media, New.

Danielewski M., 2003, Kinetics of Gaseous Corrosion Processes, Corrosion: Fundamentals, Testing, and Protection, in: ASM Handbook, Volume 13A, ASM International, Materials Park, Ohio, pp. 97-105.

Fernández F.A.P, Casteletti L.C., Totten G.E., Gallego J., 2012. Decomposition of expanded austenite in AISI 316L stainless steel nitrided at 723K, Int. Heat Treat. Surf. Eng. 6, 103-106.

Frangini S, Scaccia S. 2014. The role of foreign cations in enhancing the oxygen solubility properties of alkali molten carbonate systems: Brief survey of existing data and new research results, Int. J. Hydrogen Energy 39, 12266-12272.

Frangini S, Scaccia S., 2004. Sensitive determination of oxygen solubility in alkali carbonate melts, J. Electrochem. Soc. 151, 1251-1256.

Grabke H.J., Strauss S., Vogel D., 2003. Nitridation in NH3-H2O-mixtures, Mater. Corros. 54, 895-901.

Grabke H.J., Wolf I., 2014. Carburization and oxidation, Mater. Sci. Eng. 87, 23-33.

Hosseini S.R., Ashrafizadeh F., Kermanpur A., 2010. Calculation and experimentation of the compound layer thickness in gas and plasma nitriding of iron, Iran. J. Sci. Technol., Trans. B: Eng. 34, 553-566.

Hutchins M.G., 1983. Selective thin film coatings for the conversion of solar radiation, Surf. Technol. 20, 301-320.

Li L., 2000. AC anodization of aluminum, electrodeposition of nickel and optical property examination, Sol. Energy Mater. Sol. Cells 64, 279-289.

Mändl S., Scholze F., Neumann H., Rauschenbach B., 2003. Nitrogen diffusivity in expanded austenite, Surf. Coat. Technol. 174-175, 1191-1195.

Manova D., A. Lotnyk A., Mändl S., Neumann H. and Rauschenbach B., 2016. CrN precipitation and elemental segregation during the decay of expanded austenite, Mater. Res. Express 3, 066502, 1-15.

Manova D., Mändl S., Neumann H., Rauschenbach B., 2017. Formation of metastable diffusion layers in Cr-containing iron, cobalt and nickel alloys after nitrogen insertion, Surf. Coat. Technol. 312, 81-90.

Mehlig J.P., 1936. The determination of chromium in chromite, J. Chem. Educ. 13, 324-325.

Monteiro W.A., Lima S.A., Vatavuk J., 2017. Nitriding process characterization of cold worked AISI 304 and 316L austenitic stainless steels, J. Metall. 2017, 1-7.

Nikolussi M., Leineweber A., 2010. Mittemeijer E.J., Nitrogen diffusion through cementite layers, Philos. Mag. 90, 1105-1122.

Pettersson J, Folkeson N., Johansson L.G., Svensson J.E., 2011. The effects of KCl, K_2SO_4 and K_2CO_3 on the high temperature corrosion of a 304-type austenitic stainless steel, Oxid. Met. 76, 93-109.

Pettersson J., Froitzheim J., Pettersson C., Jonsson T., Halvarsson M., Johansson L.G., Svensson J.E., 2011. Effects of alkali salts on the high temperature corrosion of stainless steels, IFRF, Scandinavian-Nordic Section of the Combustion Institute, Pitea, Sweden.

Pye D.,2003. Practical Nitriding and Ferritic Nitrocarburizing, ASM International, Materials Park, Ohio.

Salih S.A., El-Masri A.N., Baraka A.M., 2001. Corrosion behaviour of some stainless steel alloys in molten alkali carbonates (I), J. Mater. Sci. 36, 2547-2555.

Schaaf P., Landry F., 1998. Mössbauer investigation of nitriding processes, gas nitriding and laser nitriding, in: MSMS'98, Senice, Slovakia, 1-14.

Schmalzried H., 1986. Behavior of (semiconducting) oxide crystals in oxygen potential gradients, React. Solids 1, 117-137.

Thirugnanasambandam M., et al. 2010. A review of solar thermal technologies. Renowable and sustainable energy reviews. 14, 312-322.

Tian Y., Zhao C.Y., 2013. A review of solar collectors and thermal energy storage in solar thermal applications. Applied energy 104, 538-553.

Tkacz-Śmiech K., Wierzba B., Bożek B., Danielewski M., 2016. Nitrogen diffusion and stresses during expanded austenite formation in nitriding, Defect Diffus. Forum 371, 49-58.

Vedula K., 1987. Modeling of transient and steady-state demixing of oxide solid solutions in an oxygen chemical potential gradient, Oxid. Met. 28, 99-108.

Wang J., Lin Y., Yan J., Zeng D., Huang R, Hu Z., 2012. Modification of AISI 304 Stainless Steel Surface by the Low Temperature Complex Salt Bath Nitriding at 430°C, ISIJ Int. 52, 1118-1123

Wijewardane S., Goswami D.Y., 2012. A review on surface control of thermal radiation by paints and coatings for new energy applications. Renewable and Sustainable Energy Reviews. 16, 1863–1873

Williamson D.L., Ozturk O., Glick S., Wei R., Wilbur P.J., 1991. Microstructure of ultrahigh dose nitrogen-implanted iron and stainless steel, Nucl. Instrum. Methods B 59, 737-741.

Wolf I., Grabke H.J, Schmidt P., 1988, Carbon transport through oxide scales on Fe-Cr alloys, Oxid. Met. 29, 289-306.